Desalination and Water Treatment
www.deswater.com

doi: 10.1080/19443994.2015.1131631

57 (2016) 22441–22453
October

Taylor & Francis
Taylor & Francis Group

Investigation of individual and competitive adsorption of Cu(II), Cd(II), and Pb(II) on montmorillonite in terms of surface complexation and kinetic properties of Cu(II) adsorption

Jülide Hizal[a,*], Pelin Demirçivi[a], Şeyda Karadirek[a], Reşat Apak[b]

[a]*Faculty of Engineering, Department of Chemical and Process Engineering, Yalova University, 77100 Yalova, Turkey, Tel. +90 226 8155391; Fax: +90 226 8112655; email: hizalyucesoy@yalova.edu.tr (J. Hizal), Tel. +90 226815539; Fax: +90 2268112655; email: pdemircivi@yalova.edu.tr (P. Demirçivi), Tel. +90 2268155409; Fax: +90 2268112655; email: skaradirek@yalova.edu.tr (Ş. Karadirek)*

[b]*Faculty of Engineering, Department of Chemistry, Istanbul University, Avcilar, 34320 Istanbul, Turkey, Tel. +90 2124400000; Fax: +90 2125268433; email: rapak@istanbul.edu.tr*

Received 6 March 2015; Accepted 8 December 2015

ABSTRACT

In this study, individual and competitive Cu(II), Cd(II), and Pb(II) adsorptions on montmorillonite were searched by considering surface acidic functional groups of adsorbent. pH dependency of adsorptions and kinetic properties of Cu(II) adsorption was investigated. Cu (II) adsorption on montmorillonite fits pseudo-first-order reaction with the 0.008 k value. Individual and competitive heavy metal adsorptions were modeled using Langmuir, Freundlich, Temkin, and Dubinin–Astakhov isotherms. Adsorption capacities were calculated using equations of related linearized models. The adsorption capacities of individual metal adsorption, obtained from linearized models, are higher than the yielded capacities from competitive adsorption experiments. All adsorption energies calculated from linearized Dubinin–Astakhov model varied between 7 and 16 kJ/mol. The values of adsorption energies gained for metal adsorption in competition did not significantly differ from those of individual adsorption. Since montmorillonite surface behaves as a weak acid and has a strong buffer effect at pH values between 2 and 3, the pH dependency of adsorption was explained by taking into account the surface acidic properties of adsorbent and introduced preferred surface sites beyond adsorption with increasing pH. Cu(II), Cd(II), and Pb(II) existence on loaded montmorillonite was proved by the aid of SEM-EDX results.

Keywords: Heavy metal; Montmorillonite; Adsorption; Competitive Langmuir model; Surface complexation

1. Introduction

Discharged as a waste of many industrial processes, heavy metals accumulate in soil and/or water basin. Being unbiodegradable, heavy metals may join food chain via plant and animal organisms. The EU Restriction of Hazardous Substances Directive and The EU End of Life Vehicles Directive aim to eliminate the use of hazardous chemical materials used in electric/electronic products and in the manufacture of

*Corresponding author.

new vehicles and automotive components. These directives aim to decrease the use of Pb, Cd, Hg, and Cr(VI) metals [1,2].

Activated carbon, chitosan, lignin, fly ash, and clays are commonly encountered adsorbents in various studies. In particular, clay minerals are commonly used for water treatment, because of their abundance and high affinity for both hydrophobic and hydrophilic pollutants [3–6]. The studies performed using illite and kaolin show that Cd(II) is retained more on illite than on kaolin as expected from its smectite-type structure [7]. Sciban et al. modeled Cu(II), Cd(II), and Zn(II) adsorption on wood sawdust using Langmuir, Freundlich, BET, and competitive Langmuir models. They found that the Langmuir capacities of adsorbent for individual metal adsorptions are higher than calculated from BET isotherm and observed competitive Langmuir model gives reasonable results for Cd(II) and Zn(II) competitive adsorption. High adsorption affinities of Cu(II) in both systems are attributed to paramagnetic properties of Cu(II), its higher electronegativity, and lower limiting pH of solubility. Adsorption capacities of metal cations in competition decrease in comparison with the capacities of individual adsorption. It was mentioned that Cu(II) and Zn(II) retention on surface occurs via multilayer bindings, and Cd(II) shows monolayer binding [8]. Ghorbel-Abid and Trabelsi-Ayadi studied individual and competitive Cr(III) and Cd(II) adsorption on a smectite-type clay mineral. They indicated that in competition, Cr(III) adsorption dramatically enhances, while Cd(II) adsorption decreases, and explained this situation by the fact that ionic potential and charge density of Cr(III) is higher, but electronegativity and ionic diameter are lower than Cd(II) [9]. In a recent study [10], adsorption characteristics of Pb(II), Cd(II), Cu(II) mixture on montmorillonite and Ca-montmorillonite above pH 5.5 were investigated, and it was observed that Ca-montmorillonite has more affinity for Cd(II) adsorption. In the same study, they assumed that not only unhydrolyzed metal species retain on surface, but also hydrolyzed metal species are adsorbed especially at high pH values, and surface precipitation occurred simultaneously. So, they drew species distribution diagrams for metal cations and determined dominant species at different pH intervals. In that study, concentration of working solutions varied between 0.1 and 0.005 M, and equilibrium pH values were above pH 5.5. These pH values are high enough to precipitate or hydrolyze of metal cations. To prevent surface precipitation or formation of metal-hydroxo complexes of metals, right metal concentration should be chosen as working pH [11]. As Cu(II) has the lowest limiting pH of solubility, while working with Cu(II), the maximum pH value of the solution must be 6.15 for 0.0001 M initial concentration. Otherwise, uncontrolled multilayer bindings will occur, and deviation from Langmuir isotherm appears. A similar comment can be seen in a study performed by Mihaly-Cozmuta et al. [12]. They examined pH effect on adsorption capacities of Cd^{2+}, Cu^{2+}, Co^{2+}, Mn^{2+}, Ni^{2+}, Pb^{2+}, and Zn^{2+} and showed that while approaching the limiting solubility pH of metals, adsorption capacities of metal cations dramatically enhanced.

In this study, kinetic properties of Cu(II) adsorption, individual and competitive Cu(II), Cd(II), and Pb(II) adsorptions on montmorillonite, pH dependency of adsorptions based on the surface acidity of montmorillonite are investigated. Langmuir, Freundlich, Temkin, and Dubinin–Astakhov adsorption isotherms were applied to the results of adsorption experiments. In this study, the competitive adsorption of ternary metal cation mixture is modeled using solubility-normalized Dubinin–Astakhov model for the first time. Adsorption capacities and energies of individual and competitive adsorptions were calculated from linearized equations of related models. pH dependency of adsorption is explained by considering the surface acidic properties of adsorbent and limiting pH of solubility of metal cations and introduced preferred surface sites through adsorption with increasing pH. Cu(II), Cd(II), and Pb(II) existence on loaded montmorillonite is proved by the aid of SEM-EDX results.

2. Materials and methods

2.1. Materials

Montmorillonite was received from Kale-Seramik Factory at Çanakkale. The chemical analysis of the dry adsorbents yielded the following weight percentages: SiO_2: 70.45%, Al_2O_3: 15.80%, TiO_2: 0.19%, Fe_2O_3: 1.53%, CaO: 2.02%, MgO: 2.17%, Na_2O: 0.92%, K_2O: 0.57% and loss on ignition: 6.17%. All chemicals (NaOH, HNO_3, etc.) used in the experiments were purchased from Merck. Specific surface area and particle size distribution analyses of the adsorbent were measured in previous study [13] and found that the surface area is 64 m^2/g, indicating the higher surface area of the adsorbent, 50% of the particles have a diameter of 9.24 μm, and the mean particle diameter is 12.30 μm. pH_{ZPC} value of adsorbent is estimated about pH 6. Zeta potential of montmorillonite was found to be −24.8 mV at pH 6.09.

Montmorillonite was washed with distilled water until neutral and then dried at 80°C prior to being used in the experiments.

2.2. Batch tests

Kinetic properties of metal cation adsorption were investigated for Cu(II) adsorption as a representative. Fifty milliliters of 100 ppm Cu(II) solutions was contacted with 0.5 g montmorillonite samples for 1, 2, 3, 4, 6, 12, 18, and 24 h at 25°C and at 145 rpm (Daihan Wise Shake SHO-2D orbital shaker). Capacity experiments were performed using a batch method at room temperature and constant equilibrium pH (pH 5.0 for individual and 5.1 for competitive adsorption). Heavy metal cations and their mixture solutions were prepared from their 1,000 ppm stock solutions provided that initial concentrations of working solutions vary between 50 and 600 ppm. Solid/liquid ratio was maintained at 10 g/L in all experiments. Because adsorption capacity of clays is ionic strength dependent, the ionic strength of solutions was adjusted at 0.01 M using $NaClO_4$. After filtering the suspension (Sartorius Minisart 0.45 μm filter paper), heavy metal concentrations in the filtrate were measured by flame atomic absorption spectrometer (Varian 220E FAAS), and equilibrium pH of each sample was measured with a pH-meter (WTW Inolab Level 2) equipped with a glass electrode calibrated with standard buffers. In order to search pH dependency of adsorption, 15 ppm metal solutions were treated with clays by maintaining a solid/liquid ratio at 10 g/L in the presence of 0.01 M $NaClO_4$ on a thermostatic water bath for 4 h at 25°C. The pH of each sample was adjusted in a range between 2 and 7 using 20% (by wt.) HNO_3 and 1 M NaOH. The morphologies of the loaded and unloaded samples were investigated by scanning electron microscope (SEM (JEOL Ltd., JSM-5910LV) equipped with EDS (or EDX) (OXFORD Industries INCAx-Sight 7274; 133-eV resolution 5.9 keV) after gold coating).

3. Results and discussion

3.1. Kinetic of Cu(II) Adsorption

The variation of equilibrium concentration of Cu (II) with contact time is drawn in Fig. 1(a). As observed from Fig. 1(a), 4 h of contacting is sufficient for achieving equilibrium. Kinetic of Cu(II) adsorption was investigated by the aid of pseudo-first-order model, pseudo-second-order model, and intraparticle diffusion model (Eqs. (1)–(3)).

$$\log(Q_E - Q_t) = \log Q_E - (k_1/2.303)\, t \quad (1)$$

where k_1 is the first-order rate constant, t is the contact time (min), Q_E is the adsorbed amount of Cu(II) at equilibrium, and Q_t is the adsorbed amount of Cu(II) at any time. The rate constant (k_1) can be calculated from the slope of the plot between $\log(Q_E - Q_t)$ and t (Lagergren model). A pseudo-second-order model is also used to explain the sorption kinetics. This model is expressed with the equation below (Ho and McKay Model) [14–16]:

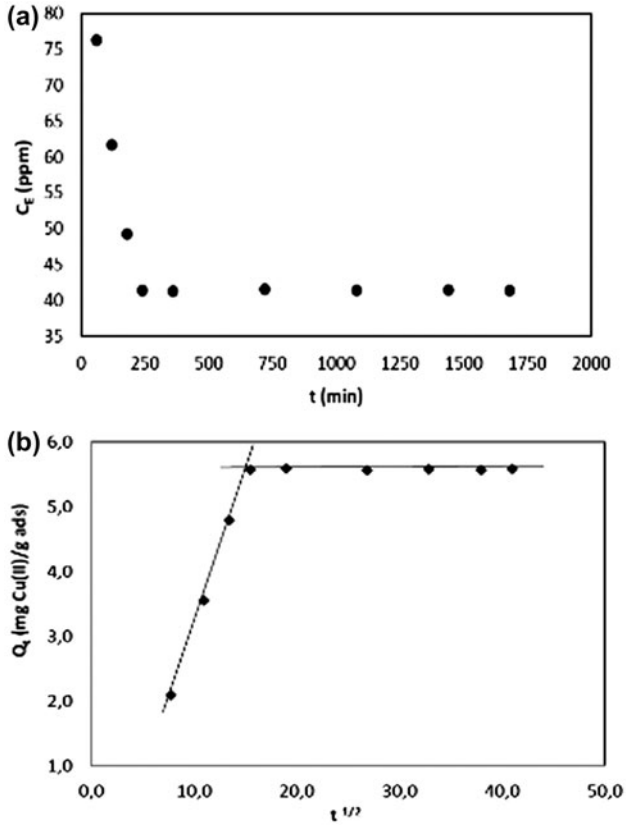

Fig. 1. (a) Time dependency of Cu(II) adsorption on montmorillonite and (b) intraparticle diffusion for the Cu(II) adsorption onto montmorillonite (for 10 g/L solid-to-liquid ratio, 0.01 mol/L $NaClO_4$).

$$t/Q_t = 1/k_2\, Q_E^2 + (1/Q_E)\, t \quad (2)$$

where k_2 is second-order rate constant and Q_E and Q_t are defined as in the pseudo-first-order model.

The mass transfer of Cu(II) in adsorption process may take place through bulk diffusion, film diffusion (boundary layer diffusion), and pore diffusion or intraparticle diffusion, respectively. Considering that the triple-layer model (TLM) is used for explaining the clay–water interface, it is said that concentration gradient between bulk solution and outer Helmholtz plane causes a migration of metal ions from bulk

solution to adsorbent surface. This migration is the fastest step of adsorption process [17–19].

Pseudo-first-order and second-order models define the bulk diffusion rate. In order to explain the boundary layer and pore diffusion rate, intraparticle diffusion model is used, and it is expressed as given below [14–16]:

$$Q_t = k_i t^{1/2} + C \quad (3)$$

where k_i is intraparticle diffusion rate constant and C is the intercept. As seen from Fig. 2(b), $t^{1/2}$ vs. Q_t curve represents a linear region. Straight line points out intraparticle diffusion. Kinetic data were also applied Bangham's model using Eq. (4):

$$\log[C_0/(C_0 - Q_t m)] = \log[(k_0 m)/(2.303\, V)] + \alpha \log t \quad (4)$$

C_0 is the initial concentration of metal cation (mol/L) V is the volume of solution (mL), m is the solid/liquid ratio (g/L), k_0 and α are the constants [16].

As observed from the Table 1, the correlation coefficient (R^2) of pseudo-second-order model is much higher than gained for pseudo-first-order model. The calculated Q_E values from the pseudo-first-order model are in good agreement with the experimental values.

3.2. Results of heavy metal adsorption experiments at fixed pH

The equilibrium pH values of the individual and competitive metal adsorption systems are 5.0 and 5.1, respectively. These pH values are under the limiting pH of solubility values for 15-600 ppm metal cation concentrations (Table 2) [11].

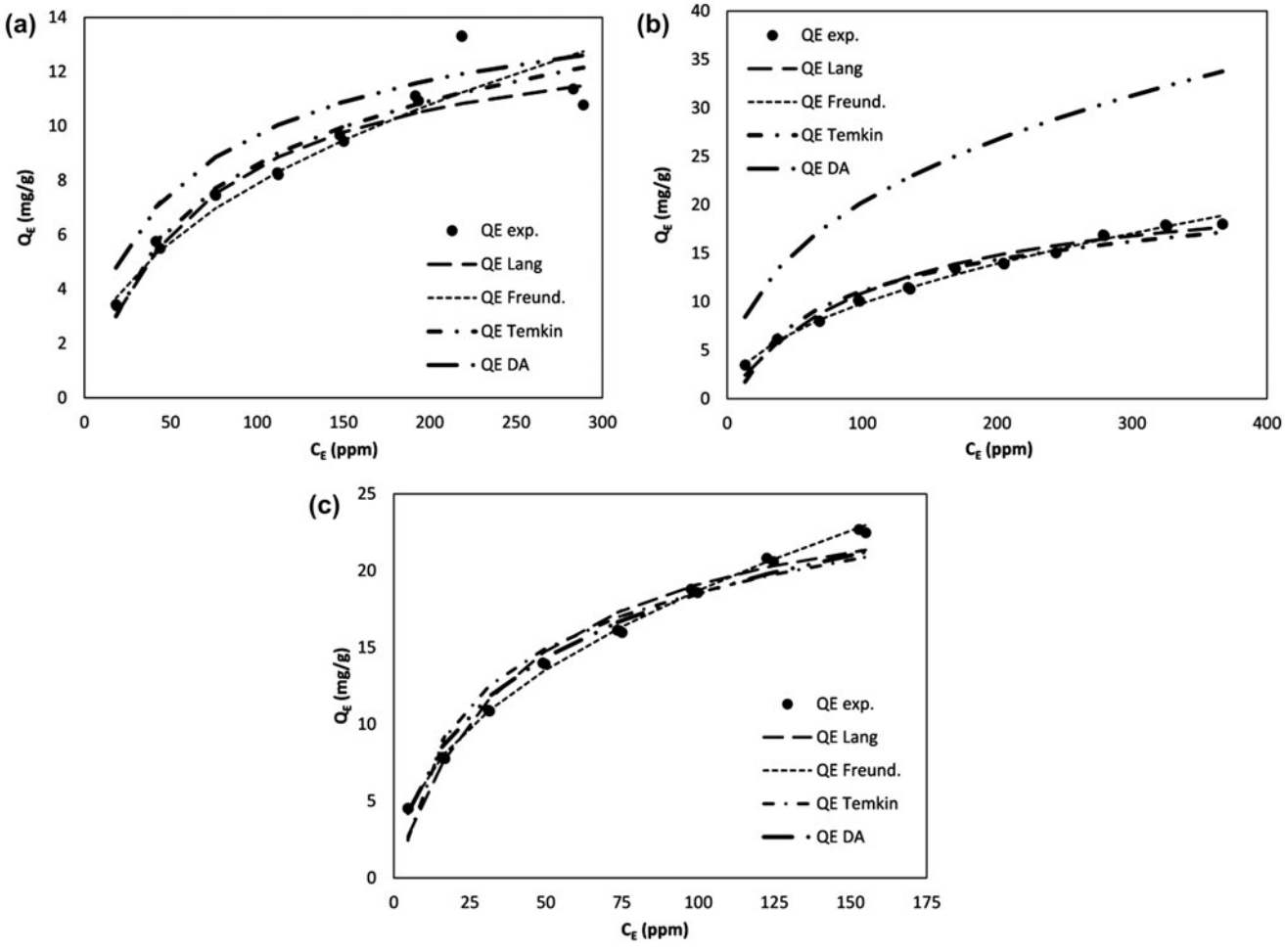

Fig. 2. Isotherm curves of individual (a) Cu(II), (b) Cd(II), and (c) Pb(II) adsorption on montmorillonite (10 g/L solid-to-liquid ratio, pH 5.0, 4 h, 0.01 mol/L $NaClO_4$).

Table 1
Applying time dependency Cu(II) adsorption results to first-order and second-order kinetic equations

	First-order kinetic parameters		Second-order kinetic parameters	
	k_1	R^2	k_2	R^2
Cu(II)	–0.0067[a]	0.928	–28.396[a]	0.846

[a]Minus values indicate exhausting of Cu(II) ions.

While determining the limiting pH of metal ion solubility, it is assumed that Cu^{2+}, $CuOH^+$, and $Cu_2(OH)_2^{2+}$ species represent Cu(II), Pb^{2+} and $PbOH^+$ species represent Pb(II), and Cd^{2+}, $CdOH^+$, and Cd_2OH^{3+} species represent Cd(II) in aqueous solution. Complexation equilibria and formation constants of metal-hydroxo complexes extracted from the literature are shown below [20–23]:

$$Cu^{2+} + H_2O \leftrightarrows CuOH^+ + H^+$$

$$\log \beta_1 = -8.22$$

$$2Cu^{2+} + 2H_2O \leftrightarrows Cu_2(OH)_2^{2+} + 2H^+$$

$$\log \beta_2 = -10.62$$

$$Pb^{2+} + H_2O \leftrightarrows PbOH^+ + H^+$$

$$\log \beta_1 = -7.70$$

$$Cd^{2+} + H_2O \leftrightarrows CdOH^+ + H^+$$

$$\log \beta_1 = -9.97$$

$$2Cd^{2+} + H_2O \leftrightarrows Cd_2OH^{3+} + H^+$$

Table 2
The limiting solubility pH for minimum and maximum heavy metal concentrations calculating from linearized equations

	pH[a]		
	15 ppm	600 ppm	$pM_t = b\ pH^a + a$
Cu(II)	5.96	5.16	$y = 1.9987x - 8.297$
Cd(II)	7.89	7.32	$y = 2.8411x - 18.525$
Pb(II)	6.20	5.39	$y = 1.9998x - 8.150$

[a]The limiting pH of solubility.

$$\log \beta_2 = -8.40$$

Data gained from isotherm experiments are applied to Langmuir, Freundlich, Temkin, and Dubinin–Astakhov models (Figs. 2 and 3). Linearized equations are shown below:

$$C_E/Q_E = 1/(K_1 \cdot Q_{max}) \cdot C_E \quad \text{(Linearized Langmuir model)} \tag{5}$$

where C_E is the equilibrium concentration of the metal ions (mg/L), Q_E is the amount of adsorbed metal ions (mg/g), Q_{max} is the maximum adsorption capacity (mg/g), K_1 is the equilibrium constant (L/mg).

$$\log Q_E = \log K_F + 1/n \log C_E \quad \text{(Linearized Freundlich model)} \tag{6}$$

where K_F and n are the Freundlich constants.

$$Q_E = B \ln A_T + B \ln C_E \quad \text{(Linearized Temkin model)} \tag{7}$$

$$B = R \cdot T/b \tag{8}$$

where A_T is the equilibrium constant of binding (L/g), B is the Temkin constant which is related to heat of sorption (J/mole), R is the gas constant (8.314 J/mole K), T is the temperature (K), and b is the Temkin Isotherm constant (unitless).

On the other hand, all isotherms are generated for gas adsorption and then adapted to solution systems. But, considering that the adsorption of metal cation occurs from aqueous solution, its solubility in water should be taken into account while modeling the metal adsorption. In this scope, solubility-normalized Dubinin–Astakhov model was used to yield the mean free energy of adsorption.

$$\ln Q_E = \ln Q_S - B_D[RT \ln (C_S/C_E)]^n \quad \text{(S-Model Linearized Dubinin–Astakhov model)} \tag{9}$$

$$B_D = 1/(E\sqrt{2})^n \tag{10}$$

where Q_S is theoretical saturation capacity (mg/g), n is the heterogeneity parameter, C_S is the solubility of metal cation (mg/L), B_D is a constant which is related to the mean free energy of adsorption (mole^2/J^2), E is the mean free energy of adsorption per mol of adsorbate (J/mole). Eq. (9) is the solubility-normalized state of Dubinin–Astakhov model [24].

The solubility concentrations of those metal cations were calculated using the equations shown in Table 2. Calculated solubility values are specific for equilibrium pH of adsorptions. The results shown in Table 3 and in Figs. 2 and 3 are yielded by taking heterogeneity factor (n) 2, which produces good correlation coefficient values.

Conformity of applied isotherms with experimental data is searched by the aid of coefficient of determination (R^2) (Eq. (11)) and chi-square values (χ^2) (Eq. (12)).

$$R^2 = \left[\sum \left(Q_{cal} - Q_{aexp}\right)^2\right] / \left[\sum \left(Q_{cal} - Q_{aexp}\right)^2 + \left(Q_{cal} - Q_{exp}\right)^2\right] \quad (11)$$

$$\chi^2 = \sum \left[\left(Q_{cal} - Q_{exp}\right)^2 / Q_{cal}\right] \quad (12)$$

Unlike the work presented in the literature [25–27], competition of Cu(II), Cd(II), and Pb(II) was investigated for ternary adsorptive ion systems by considering their solubilities.

Table 3 shows that individual Cd(II) and Pb(II) adsorptions fit to Freundlich model (Figs. 2 and 3 also support this outcome), whereas they show Langmuirian character during adsorption from their mixture solution. This situation conforms with the literature knowledge that explains Cu(II), Cd(II), Pb(II), and Ni(II) competitive adsorptions on clay are better fitted with the Freundlich model [28]. On the other hand, individual and competitive Cu(II) adsorption can be explained by Temkin model which gives better conformity. Unlike the Langmuir Isotherm, Temkin and Freundlich models consider molecular interactions between adsorbates. Thus, it can be said that individual adsorptions of each metal cations occur as a result of these interactions. Because Cu(II) gives more stable complexes with O-donor ligands, dominant adsorptive cation must be Cu(II) ions. This assumption explains unchanged adsorption character of Cu(II) during competitive adsorption. As being a Lewis acid, when Cu(II) reacts to form octahedral complex, the structure is subjected to Jahn-Teller effect. This effect gives an extra stability to Cu(II) complexes. For high-spin complexes of the divalent heavy metal ions, the stability constant of complex follows the order of Mn(II) < Fe(II) < Co(II) < Ni(II) < Cu(II) > Zn(II) [29]. High adsorption capacity of Pb(II) and Cu(II) can be explained by forming stable complexes with –OH groups of hydrated silica and alumina using HSAB (Hard and Soft Acids and Bases Theory) theory. Jiang et al. found that the Pb(II) cations had the higher adsorption on kaolinite and attributed this situation to stronger preference of kaolinite surface for Pb(II) than others [28]. Though individually adsorbed Cd(II) and Pb(II) ions in accord with Freundlich isotherm, which considers intermolecular bindings, their competitive adsorptions show Langmuirian character. Taking into account Langmuir assumptions which estimates monolayer binding on the adsorbent surface, it can be said that dominant Cu(II) adsorption inhibits the interaction between adsorbed Cd(II) and Pb(II) species and forces them to monolayer binding. As seen from Table 3, the maximum adsorption capacities of Cd(II) and Pb(II) ions significantly decrease in competition. In competition, the sum of maximum adsorption capacity values of whole metal cations equal 0.287 mmol/g, and this value is quite close to that achieved in individual Cu(II) adsorption (0.223 mmol/g). It is thought that this situation arises from surface sites of adsorbent being shared among heavy metal cations.

Going on observing the Table 3, it can be seen that maximum adsorption of Cd(II) on montmorillonite is higher than maximum adsorption of Pb(II), and it is almost close to Cu(II) adsorption capacity. Previous

Table 3
Individual and competitive adsorption capacities(mmol g^{-1}) of Cu(II), Cd(II), and Pb(II) cations onto montmorillonite, Langmuir and Freundlich parameters([$NaClO_4$] = 0.01 M)

		Langmuir parameters			Freundlich parameters		Q_{max} calculated from Butler and Ockrent's extended Langmuir model	
		Equation	Q_{max}	R^2	Equation	R^2		R^2
Individual	Cu(II)	$y = 0.071x + 4.586$	0.223	0.981	$y = 0.451x - 0.006$	0.971	–	–
	Cd(II)	$y = 0.043x + 4.941$	0.205	0.973	$y = 0.501x - 0.009$	0.997	–	–
	Pb(II)	$y = 0.037x + 1.483$	0.131	0.971	$y = 0.466x + 0.340$	0.999	–	–
In mixture	Cu(II)	$y = 0.102x + 4.374$	0.154	0.973	$y = 0.326x + 0.142$	0.934	0.035	
	Cd(II)	$y = 0.124x + 7.220$	0.072	0.989	$y = 0.359x - 0.043$	0.962	0.058	
	Pb(II)	$y = 0.079x + 3.231$	0.061	0.992	$y = 0.374x + 0.160$	0.944	0.025	

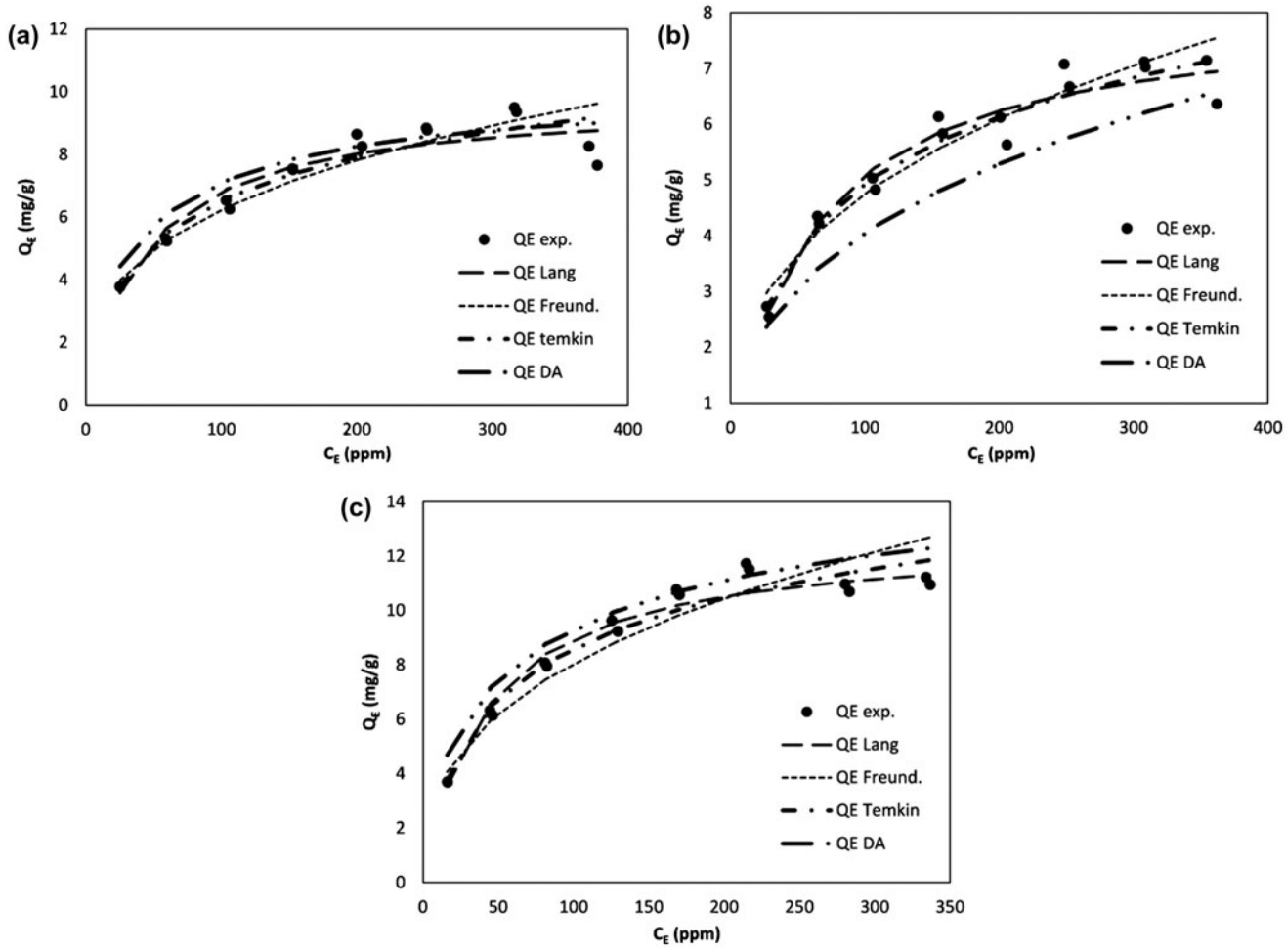

Fig. 3. Isotherm curves of competitive (a) Cu(II), (b) Cd(II), and (c) Pb(II) adsorption on montmorillonite (10 g/L solid-to-liquid ratio, pH 5.1, 4 h, 0.01 mol/L $NaClO_4$).

studies showed that unlike from Cu(II) and Pb(II) adsorption, Cd(II) adsorption enhances with decreasing ionic strength of suspension [30–32]. This situation is explained by Cd(II) retention on permanently negatively charged (on silica surfaces) sites which occurred as a result of isomorphic substitution and priorly occupied with Na^+ ions of inert electrolyte [30]. In this study, 2:1 smectite-type structure of montmorillonite causes significant enhancement in Cd(II) adsorption because of its high affinity to negatively charged surface.

Comparing the maximum adsorption capacities yielded from Langmuir and Solubility-Normalized Dubinin–Astakhov models, the calculated Q_{max} values are quite close to each other for Cu(II) and Pb (II) adsorptions. On the other hand, the maximum capacities of Cd(II) ions calculated by Solubility-Normalized DA model are significantly higher than the values obtained from Langmuir model. Solubility-Normalized DA model considers solubility of adsorbate. The limiting pH of Cd(II) is higher than limiting pH values of Cu(II) and Pb(II) ions. These two reasons lead to an expectation of higher adsorption capacity from Cd(II) cations. Cd(II) ion can exist unhydrolyzed metal ion (Cd^{2+}) until pH 7. But the working pH of isotherm experiments was adjusted at limit pH to prevent surface precipitation of Cu(II) ions. As observed from Figs. 4–6, despite of 80% adsorption of Cu(II) and Pb(II), 60% of Cd(II) is adsorbed on the surface at pH 5. Thus, this situation may lead to a lower gain adsorption capacity than expected.

The mean free energy values calculated from DA Model vary between 7 and 16 kJ/mol, which indicate an ion exchange process [33].

3.3. pH-dependent adsorption of Cu(II), Cd(II), and Pb(II)

Fig. 7 shows that even after half of the total base volume is exhausted, the pH of system does not significantly change. This pH resistant region shows a strong buffer effect on adsorbent resulting from deprotonation of permanently negatively charged surface of 1:1 or 2:1 clay minerals [30,31]. In spite of adding more base, steep surge was not observed through alkalimetric titration. If the axes switch, this pH region (between 3 and 9) indicates a plateau region where ≡SOH species is dominant. And it means the clay surface behaves as a weak acid. Upon further examination of titration curve, it can be said that pH_o value of montmorillonite is around 6. This is in good agreement with Tombacz' s expression which characterized the edges OH groups having pH_o ~ 6.5 as less basic than the Al–OH and less acidic than the Si–OH groups [34]. So, at lower pHs than pH ~ 6.5, while silica sites are deprotonated, alumina sites still maintain its protonated form. At higher pH values, both silica and alumina sites are negatively charged. According to Kosmulski, PZC value of montmorillonite can vary between 3 and 9 depending on the source of montmorillonite and whether the sample is Na- or K-montmorillonite [35].

pH-dependent experiments show that the adsorbed amount of metal cation increases with increasing pH. In individual metal adsorption, the maximum adsorptions are achieved in a range of $3.5 < pH < 5.5$ for Cu (II), $3 < pH < 6$ for Pb(II), and $3 < pH < 7$ for Cd(II) (Figs. 4–6). Increasing pH trend of metal adsorption is parallel to limiting pH of solubility of metal cations (Table 1). The maximum adsorption of more than one heavy metal cation from same solution occurs at pH values between 3 and 6. All these situations can be explained by the fact that zero point of charge of adsorbent is around pH 6, and the charge density of surface dramatically changes beyond this pH interval.

Wide pH range (nearly $3 < pH < 7$) for achieving maximum adsorption capacity indicates retention on more than one surface sites of montmorillonite. The metal ion is partly hydrolyzed but still retains its

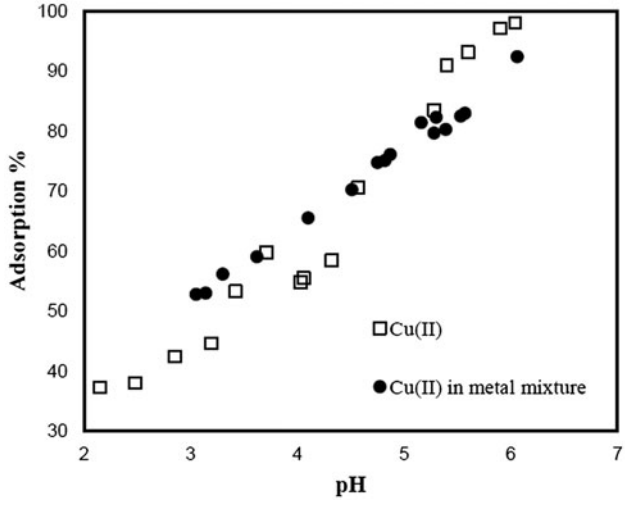

Fig. 4. Adsorption % vs. pH curves for individual and competitive Cu(II) adsorption on montmorillonite (15 ppm metal solutions and a solid/liquid ratio of 10 g/L in the presence of 0.01 mol/L $NaClO_4$).

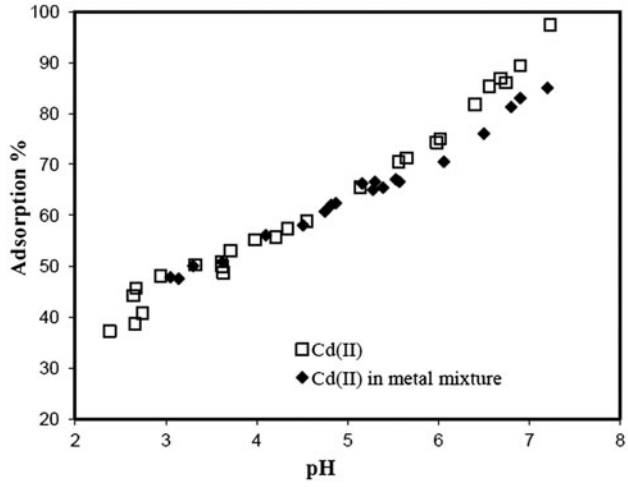

Fig. 5. Adsorption % vs. pH curves for individual and competitive Cd(II) adsorption onto montmorillonite (15 ppm metal solutions and a solid/liquid ratio of 10 g/L in the presence of 0.01 mol/L $NaClO_4$).

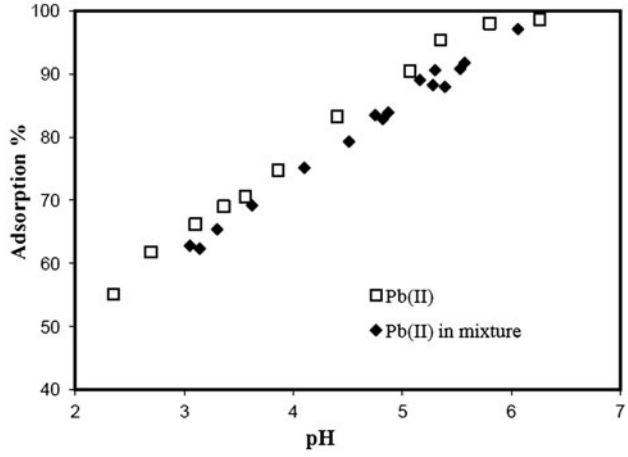

Fig. 6. Adsorption % vs. pH curves for individual and competitive Pb(II) adsorption onto montmorillonite (15 ppm metal solutions and a solid/liquid ratio of 10 g/L in the presence of 0.01 mol/L $NaClO_4$).

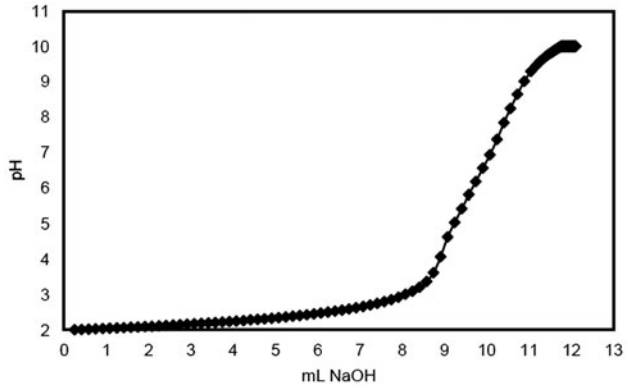

Fig. 7. Alkalimetric titration curve of montmorillonite formerly titrated with 0.1 N HCl (Suspension conc.: 10 g/L, titration rate: 2 mL/min, [$NaClO_4$] = 0.01 M, [NaOH] = 0.1 N) [20]

positive charge in this pH range. On the other hand, the clay surface has a negative charge because the pH is higher than PZC. So, it can be said that adsorption occurs by interaction between negatively charged clay surface and positively charged M^{2+} which can be define as physisorption.

In competition, Cu(II) adsorption shows an increase at lower pH values and a decrease with increasing pH, compared with individual adsorption. While Cd(II) adsorption reduces at higher pH, Pb(II) adsorption shows same trend with individual adsorption. pH vs. adsorption% curves of Cu(II) and Pb(II) adsorptions do not include 100% adsorption data points higher than pH 6 because of decreasing solubility.

3.4. Definition of surface-metal complexation

Inspection of pH vs. adsorption% graphs (Figs. 4–6) and titration curve (Fig. 7) shows that the surge region in alkalimetric titration curve and pH interval at which maximum adsorption of metal ions achieve are located in the same pH region. Assuming PZC of montmorillonite is around pH 6, dominant species below pH 6 (mostly alumina surfaces) are positively charged, while other species (mostly silica sites) are negatively charged. On the other hand, all surface species are negatively charged above pH 7. In previous studies, surface sites of kaolin-type clay minerals were defined by the presence of silica (symbolized as $\equiv S_1OH$); alumina ($\equiv S_2OH$), and permanently negatively charged (X^-) surface occurred as a result of isomorphic substitution. These studies also showed that binding to surface took place by forming inner- and/or outer-sphere binary complexes between surface and M^{2+} ion [30,31,36,37]. Possible reactions for heavy metal cation (M^{2+}) retention are listed below:

$$\equiv S_1OH + M^{2+} \leftrightarrows \equiv S_1OM^+ + H^+ \quad K_1$$

$$\equiv S_2OH + M^{2+} \leftrightarrows \equiv S_2OM^+ + H^+ \quad K_2$$

$$2NaX + M^{2+} \leftrightarrows MX_2 + 2Na^+ \quad K_3$$

K_3 equilibrium dominates at pH values between 2 and 3. In this pH region, both silica and alumina sites are in their diprotic form ($\equiv SOH^{2+}$). So, they cannot interact with unhydrolyzed metal cation. Above pH 3, silica surface, respectively, becomes neutral and negatively charged, but alumina surface is still positively charged until pH around 7. At these pH values unhydrolyzed M^{2+} forms inner-sphere binary complex with silica surface sites (K_1 equilibrium). While alumina sites ($\equiv S_2OH$) get negatively charged, heavy metal cation simultaneously binds to surface via forming inner-sphere binary complex (K_2 equilibrium), and this reaction is dominant because of being a stronger Lewis base than silica. All these reactions occur via ion exchange process. The increase in adsorption percentage with increasing pH and mean free energy values (between 7 and 16 kJ/mol) support this consequence. These results are in consistent with the introduced by Schaller et al. for Cd(II) adsorption [32]. Unlike from Benyahya and Garnier [38], Schaller et al. considered the permanent negatively charged surface in addition to the pH-dependent edge sites. They modeled the Cd(II) adsorption on kaolinite using double-layer model and showed that the dominant species responsible from adsorption are ion exchange sites of kaolinite. Their considerations and results are in good agreement with literature knowledge [31]. On the other hand, Abate et al. mentioned that the major process for Cd(II) adsorption on vermiculite is ion exchange, while that of Pb(II) is complexation [37].

3.5. SEM images and EDS spectrums of loaded and unloaded montmorillonite

As seen from Figs. 8(a)–(e) which show 100 times zoomed SEM images and EDS spectrums, Si, Al, Fe, K, Mg, Ca elements contained by montmorillonite structure appear in EDS spectrums. The spectrums of heavy metal loaded montmorillonite samples additionally include Cu, Cd, and Pb elements. So, SEM-EDX results proved Cu(II), Cd(II), and Pb(II) existence on loaded montmorillonite.

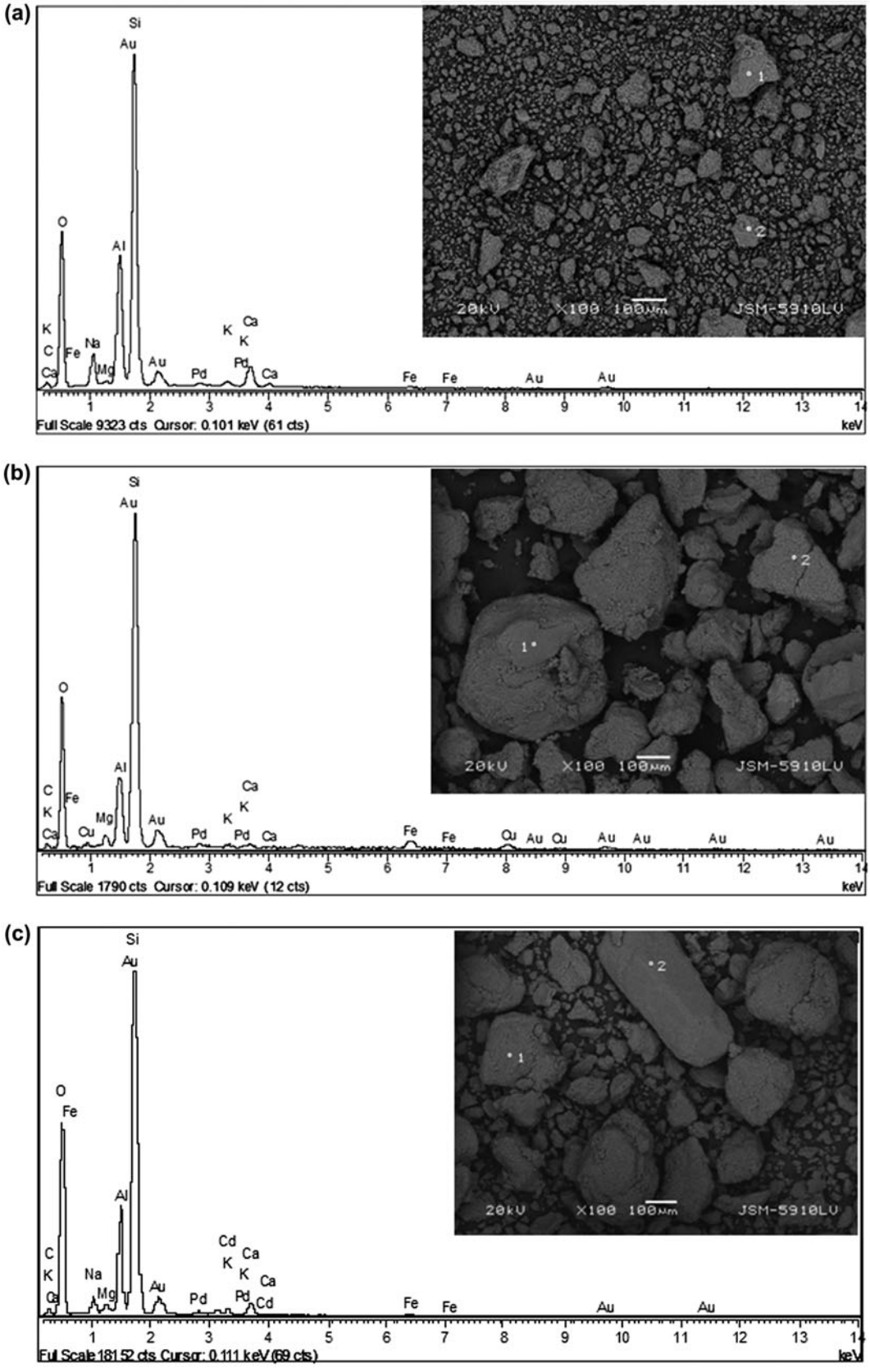

Fig. 8. SEM image and EDS spectrum of (a) unloaded, (b) Cu(II) loaded, (c) Cd(II) loaded, (d) Pb(II) loaded, (e) Cu(II), Cd(II), and Pb(II) loaded montmorillonite ([$NaClO_4$] = 0.01 mol/L, t = 4 h, fixed pH, solid/liquid ratio of 10 g/L).

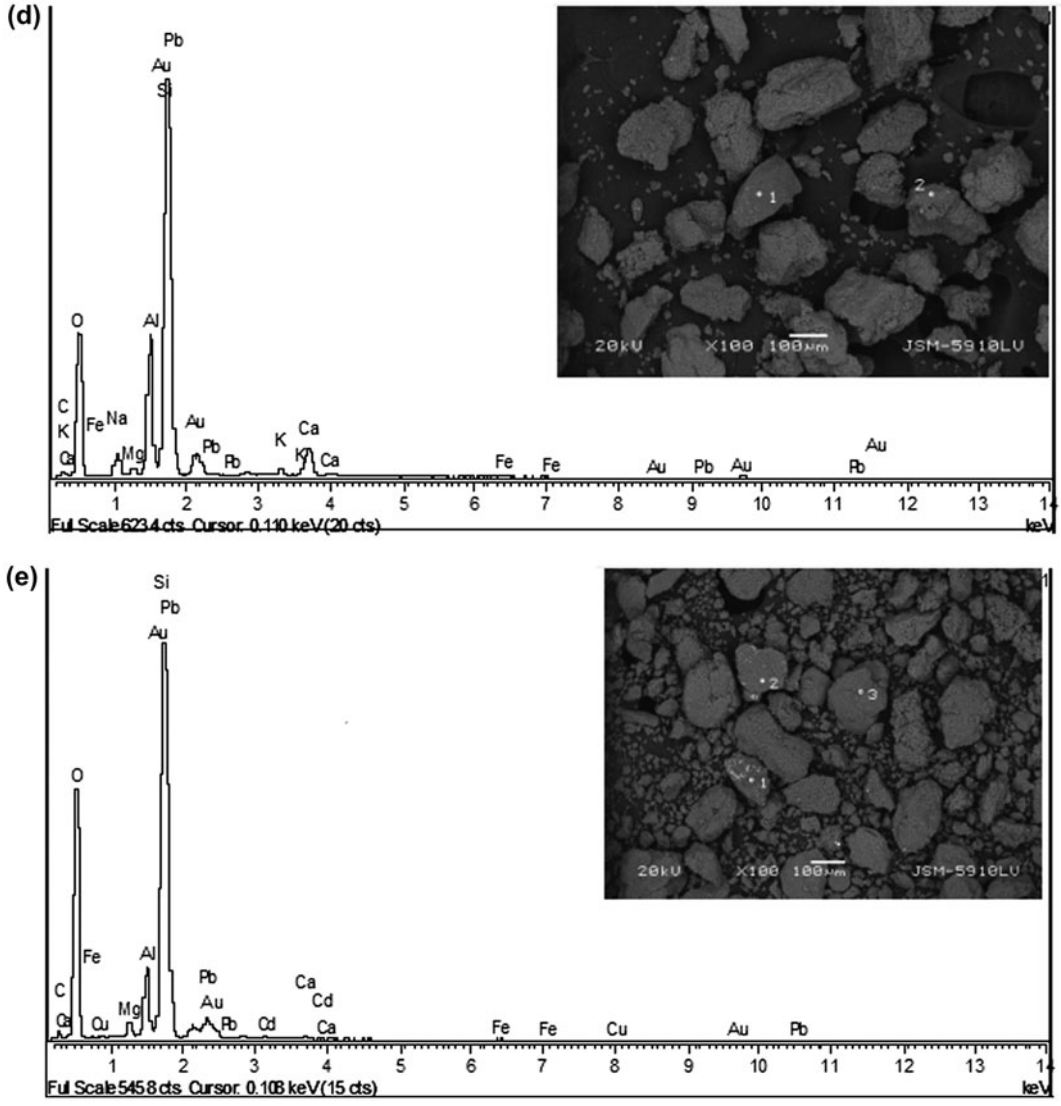

Fig. 8. (*Continued*).

4. Conclusion

Montmorillonite surface behaves as a weak acid and has a strong buffer effect at pH values between 2 and 3. Point of zero charge of montmorillonite is around pH 6. These acidic properties of surface are decisive parameters for heavy metal adsorption on surface. The kinetic of heavy metal adsorption on montmorillonite fits pseudo-first-order reaction. While individual adsorptions refer to intermolecular binding between adsorbed species for all metal cations, in competition Cu(II) ions manage the adsorption process by maintaining its molecular interactions and forcing Pb(II) and Cd(II) to monolayer binding. Cu(II) has the highest individual and competitive adsorption capacity because of being a stronger Lewis acid and having Jahn-Teller effect. 2:1 smectite-type structure of montmorillonite causes significant enhancement in Cd (II) adsorption because of its high affinity to negatively charged surface. Competition among metal cations reduces the adsorbed amount of cations while adsorption characteristic is maintained. That the maximum adsorption is achieved at nearly pH between 3 and 7, and this shows metal cations are retained on more than one surface sites on montmorillonite. Adsorption occurs by interaction between negatively charged clay surface and positively charged M^{2+} via an ion exchange process. The mean free energy values also support this conclusion. At pH values between 2

and 3, metal adsorption mostly occurs via interaction between permanently negatively charged silica surfaces. At pH values between 3 and 7, metal cation binds to silica surface to form inner-sphere binary complex. Above pH 7, the formation of inner-sphere binary complex between alumina surface sites and unhydrolyzed metal cation is the dominant adsorption mechanism.

Acknowledgment

The authors wish to express their gratitude to Re&De Department of Kale-Seramik Co. (Ceramic Factory at Çanakkale) for providing the montmorillonite samples.

References

[1] The European Union (EU) End of Life Vehicles (ELV), Directive 2000/53/EC, p. 8.
[2] The European Union (EU) Restriction of the use of certain Hazardous Substances(RoHS), Directive 2002/95/EC, p. 1.
[3] K. Lackovic, M.J. Angove, J.D. Wells, B.B. Johnson, Modeling the adsorption of Cd(II) onto Muloorina illite and related clay minerals, J. Colloid Interface Sci. 257 (2003) 31–40.
[4] D.P.H. Laxen, Cadmium adsorption in freshwaters—A quantitative appraisal of the literature, Sci. Total Environ. 30 (1983) 129–146.
[5] L.M. Shukla, Sorption of zinc and cadmium on soil clays, Agrochimica 44 (2000) 101–106.
[6] H. Halen, R. Van Bladel, P. Cloos, Relation pH-adsorption du cuivre, du zinc et du cadmium pour quelques sols et minéraux argileux (pH-adsorption relationship for adsorption of copper, zinc, and cadmium onto soils and clay minerals), Pedologie 41 (1991) 47–68.
[7] A.G. Sanchez, E. Ayuso, O. Blas, Sorption of heavy metals from industrial waste water by low-cost mineral silicates, Clay Miner. 34 (1999) 469–469.
[8] M. Šćiban, B. Radetić, Ž. Kevrešan, M. Klašnja, Adsorption of heavy metals from electroplating wastewater by wood sawdust, Bioresour. Technol. 98 (2007) 402–409.
[9] I. Ghorbel-Abid, M. Trabelsi-Ayadi, Competitive adsorption of heavy metals on local landfill clay, Arab. J. Chem. 8 (2011) 25–31.
[10] L. Pablo, M.L. Chávez, M. Abatal, Adsorption of heavy metals in acid to alkaline environments by montmorillonite and Ca-montmorillonite, Chem. Eng. J. 171 (2011) 1276–1286.
[11] R. Apak, J. Hizal, C. Ustaer, Correlation between the limiting pH of metal ion solubility and total metal concentration, J. Colloid Interface Sci. 211 (1999) 185–192.
[12] L. Mihaly-Cozmuta, A. Mihaly-Cozmuta, A. Peter, C. Nicula, H. Tutu, D. Silipas, E. Indrea, Adsorption of heavy metal cations by Na-clinoptilolite: Equilibrium and selectivity studies, J. Environ. Manage. 137 (2014) 69–80.
[13] A. Erçağ, P. Demirçivi, J. Hizal, Kinetic, isotherm and ph dependency investigation and environmental application of cationic dye adsorption on montmorillonite, Desalin. Water Treat. 56 (2014) 2447–2456
[14] P. Sivakumar, N. Palanisamy, Mechanistic study of dye adsorption onto a novel non-conventional low-cost adsorbent, Adv. Appl. Sci. Res. 1 (2010) 58–65.
[15] M. Gouamid, M.R. Ouahrani, M.B. Bensaci, Adsorption equilibrium, kinetics and thermodynamics of methylene blue from aqueous solutions using date palm leaves, Energy Procedia 36 (2013) 898–907.
[16] C.Y. Kuo, C.H. Wu, J.Y. Wu, Adsorption of direct dyes from aqueous solutions by carbon nanotubes: Determination of equilibrium, kinetics and thermodynamics parameters, J. Colloid Interface Sci. 327 (2008) 308–315.
[17] M.J. Avena, C.P. De Pauli, Modeling the interfacial properties of an amorphous aluminosilicate dispersed in aqueous NaCl solutions, Colloids Surf., A: Physicochem. Eng. Aspects 118 (1996) 75–87.
[18] M.J. Avena, C.P. De Pauli, Proton adsorption and electrokinetics of an argentinean montmorillonite, J. Colloid Interface Sci. 202 (1998) 195–204.
[19] J. Gonçalvès, P. Rousseau-Gueutin, A. Revil, Introducing interacting diffuse layers in TLM calculations: A reappraisal of the influence of the pore size on the swelling pressure and the osmotic efficiency of compacted bentonites, J. Colloid Interface Sci. 316 (2007) 92–99.
[20] S. Goldberg, Adsorption models incorporated into chemical equilibrium models, in: R.H. Leoppert, A.P. Schwab, S. Goldberg (Eds.), Chemical Equilibrium and Reaction Models, SSSA-ASA special publication, Madison, WI, 1995, pp. 75–97.
[21] C. Ludwig, P.W. Schindler, Surface complexation on TiO_2: I. Adsorption of H^+ and Cu^{2+} ions onto TiO_2 (Anatase), J. Colloid Interface Sci. 169 (1995) 284–290.
[22] C. Ludwig, P.W. Schindler, Surface complexation on TiO_2, J. Colloid Interface Sci. 169 (1995) 291–299
[23] P.J. Pretorius, P.W. Linder, The adsorption characteristics of δ-manganese dioxide: A collection of diffuse double layer constants for the adsorption of H^+, Cu^{2+}, Ni^{2+}, Zn^{2+}, Cd^{2+} and Pb^{2+}, Appl. Geochem. 16 (2001) 1067–1082.
[24] V.J. Inglezakis, Solubility-normalized Dubinin–Astakhov adsorption isotherm for ion-exchange systems, Microporous Mesoporous Mater. 103 (2007) 72–81.
[25] O. Dusart, S. Souabi, M. Mazet, Elimination of surfactants in water treatment by adsorption onto activated carbon, Environ. Technol. 11 (1990) 721–730.
[26] C. Faur, H.M. Pignon, P. Le Cloirec, Multicomponent adsorption of pesticids onto, acticated carbon fibers, Adsorption 11 (2005) 479–490.
[27] F. Pagnaneli, Equilibrium, kinetic and dynamic modeling of biosorption processes, in: P. Kotrba, M. Mackova, T. Macek (Eds.), Microbial Biosorption of Metals (2001) 59–120
[28] M. Jiang, X. Jin, X.Q. Lu, Z. Chen, Adsorption of Pb (II), Cd(II), Ni(II) and Cu(II) onto natural kaolinite clay, Desalination 252 (2010) 33–39.
[29] H.M.N.H. Irving, R.J.P. Williams, The stability of transition-metal complexes, J. Chem. Soc. 3 (1953) 3192–3210.
[30] J. Hizal, R. Apak, Modeling of copper(II) and lead(II) adsorption on kaolinite-based clay minerals individually and in the presence of humic acid, J. Colloid Interface Sci. 295 (2006) 1–13

[31] J. Hizal, R. Apak, Modeling of cadmium(II) adsorption on kaolinite-based clays in the absence and presence of humic acid, Appl. Clay Sci. 32 (2006) 232–244
[32] M.S. Schaller, C.M. Koretsky, T.J. Lund, C.J. Landry, Surface complexation modeling of Cd(II) adsorption on mixtures of hydrous ferric oxide, quartz and kaolinite, J. Colloid Interface Sci. 339 (2009) 302–309.
[33] E.B. Simsek, E. Özdemir, U. Beker, Zeolite supported mono- and bimetallic oxides: Promising adsorbents for removal of As(V) in aqueous solutions, Chem. Eng. J. 220 (2013) 402–411.
[34] E. Tombácz, M. Szekeres, Colloidal behavior of aqueous montmorillonite suspensions: The specific role of pH in the presence of indifferent electrolytes, Appl. Clay Sci. 27 (2004) 75–94.
[35] M. Kosmulski, The pH dependent surface charging and points of zero charge, J. Colloid Interface Sci. 353 (2011) 1–15.
[36] D. Arda, J. Hizal, R. Apak, Surface complexation modeling of uranyl adsorption onto kaolinite based clay minerals using FITEQL 3.2, Radiochim. Acta 94 (2006) 835–844.
[37] G. Abate, J.C. Masini, Influence of pH, ionic strength and humic acid on adsorption of Cd(II) and Pb(II) on vermiculite, Colloids Surfaces A 262 (2005) 32–39.
[38] L. Benyahya, J.M. Garnier, Effect of salicylic acid upon trace-metal sorption (CdII, Zn II, Co II, and MnII) onto alumina, silica, and kaolinite as a function of pH, Environ. Sci. Technol. 33 (1999) 1398–1407.